ABUAD Journal of Engineering and Applied Sciences (AJEAS)

ISSN: 2992-5584

Volume 3, Issue 1, 11-18

# Silver Nanoparticles Recovery from X-ray Films using Humic and Fulvic Acids: Synthesis and Antimicrobial Applications

Owolabi Mutolib BANKOLE[1*], Temitope Michael ALADEJANA[2], Julius Gbenga OMOSEBI[3], Abiola Olanike ADESINA[1], Segun Esan OLASENI[1]

[1*]*Department of Chemical Sciences, Adekunle Ajasin University, Akungba, Nigeria*
[2]*Microbiology Unit, Science Technology Department, Federal Polytechnic, Ado-Ekiti, Nigeria*
[3]*Chemistry Unit, Science Technology Department, Federal Polytechnic, Ado-Ekiti, Nigeria*

[1]owolabi.bankole@aaua.edu.ng, [2]aladejana684@gmail.com, [3]omosebi_jg@fedpolyado.edu.ng, [1]abiola.adesina@aaua.edu.ng, [1]lincolnolaseni@yahoo.com

[*]Correspondence: owolabi.bankole@aaua.edu.ng, bankolemutolib@yahoo.com; Tel.:+2348034018955

*Date Submitted:* 14/02/2025
*Date Accepted:* 20/05/2025
*Date Published:* 30/06/2025

*Abstract***:** *The current study investigates the recovery and synthesis of silver nanoparticles (AgNPs) from used x-ray photographic films as a sustainable and cost-effective strategy for scalable production. Silver was extracted using an alkaline NaOH solution and stabilised with humic (HA) and fulvic (FA) acids, demonstrating a green chemistry approach that enhances nanoparticle stability and biocompatibility. FTIR analysis confirmed the incorporation of functional groups for AgNP stabilisation, SEM revealed well-dispersed nanoparticles, and XRD verified their crystalline structure. The HA- and FA-stabilised AgNPs showed superior antimicrobial activity compared to pure AgNPs, with inhibition zones of 35 and 39 mm against Escherichia coli and Streptococcus pneumonia, respectively. The antibacterial effects of the synthesised particles were found to be concentration-dependent. This dual approach of waste photographic film valorisation and in situ nanoparticle stabilisation offers an eco-friendly pathway for functional AgNP production with potential applications in medical and environmental fields.*

***Keywords:*** Silver nanoparticles, x-ray film recycling, humic and fulvic acid stabilization, green synthesis, antimicrobial activity.

## 1. INTRODUCTION

Silver and its nanoparticle derivatives are widely recognized for their potent activity against diverse microbial pathogens [1, 2], which makes them valuable in medical, environmental, and industrial applications [3, 4]. Traditional methods for synthesizing AgNPs often require expensive precursors and complex processes, which limit their large-scale production and sustainable application [5]. In recent years, the recovery and synthesis of AgNPs from waste materials, such as used x-ray photographic films, have gained attention as a cost-effective and environmentally friendly alternative and a sustainable approach to mitigate resource depletion while exploring new, cost-effective avenues for nanoparticle synthesis. These X-ray films contain silver in their Gelatin layers, providing a valuable source of recoverable AgNPs, and their utilization addresses both waste management and resource recovery challenges, aligning with the broader goals of green chemistry by reducing waste and promoting resource circularity [6, 7].

The process of extracting AgNPs from X-ray films involves treating the gelatin-silver layers with an alkaline solution, with sodium hydroxide promoting gelatin matrix dissolution and subsequent release of silver ions. This method has been shown to effectively recover silver while minimizing environmental impact [8]. In the current study, humic (HA) and fulvic (FA) acids, two naturally occurring organic substances, are employed as stabilizing agents for the synthesized AgNPs. Both HA and FA are rich in functional groups that can chelate and stabilize metal ions, making them suitable for supporting the formation of AgNPs with enhanced stability and biocompatibility [9, 10]. By using these natural stabilizers, this approach not only enables the sustainable recovery of silver but also integrates the antimicrobial properties of both the AgNPs and the organic acids, potentially broadening the utility of the recovered nanoparticles [11].

While there are existing methods for recovering silver from X-ray films [9, 12, 13] most focus on chemical leaching without producing silver in a stabilized nanoparticulate form suitable for direct applications [14]. This novelty of the current study lies in combining silver recovery with the in-situ stabilization of AgNPs using natural organic matter, specifically humic acid (HA) and

fulvic acid (FA). The resulting stabilized AgNPs are particularly valuable for direct applications, especially for antimicrobial use, given the well-documented broad-spectrum antimicrobial properties of silver nanoparticles [15, 16]. These organic compounds, rich in functional groups, provide an eco-friendly stabilization route, supporting the creation of AgNPs with enhanced dispersion and stability, a feature often overlooked in previous work [17]. This dual recovery and stabilization approach represents a green chemistry solution that integrates waste valorisation with nanoparticle synthesis and provides a pathway to reduce the environmental impact of AgNP production.

The strong antimicrobial properties of AgNPs are well-recognized; however, consistent stability and bioavailability in real-world applications continue to be limiting factors. The present study addresses this gap by harnessing the unique structural and functional properties of HA and FA to not only stabilize but also potentially augment the antimicrobial efficacy of AgNPs. This work contributes to the field by filling research gaps in nanoparticle recovery from waste materials with integrated stabilization using natural compounds, highlighting a practical, low-cost, and sustainable method for developing multifunctional AgNPs suitable for medical and environmental applications. This work thus opens up new possibilities for sustainable AgNP synthesis, contributing to both waste management and antimicrobial material innovation.

## 2. Materials and Method

### 2.1 Materials

The reagents used in this study were commercially sourced and used as received, with no further purification: D-(+)-Glucose monohydrate ($C_6H_{12}O_6 \cdot H_2O$, Zhengzhou Alfa Chemical, China), Humic acid sodium salt (Technical, Zhengzhou Alfa Chemical, China), absolute ethanol (99.9%), and sodium hydroxide (flakes, Sigma-Aldrich, $\geqslant$ 98.0%). De-ionized water (18 MΩ) was supplied by Pascal Scientific, Nigeria. Used x-ray photographic films were graciously received from Ondo State Specialist Hospital, Ikare-Akoko, Ondo State, Nigeria.

### 2.2 Material Preparation

#### *2.2.1 Processing of x-ray photographic films*

The used x-ray films were cleaned by washing under tap water, followed by distilled water to remove the surface dirt and contaminants, then dried using a clean paper towel. To eliminate residual organic impurities, the films were soaked in ethanol for 2 min, effectively removing oils and organic residues. After cleaning, the films were cut into uniform strips measuring approximately 2 cm x 2 cm before undergoing further extraction and leaching of the gelatin silver layers.

#### *2.2.2 Preparation of AgNPs from x-ray films using NaOH*

To obtain uncoated AgNPs from the used X-ray films, 10 g of X-ray films were dispersed in NaOH solution (100 mL, 1.5 M) and the resulting mixture was heated to 90 °C for 30 min. The complete leaching of Ag from the X-ray films was indicated by a colour change in the gelatin films from black to clear blue, indicating the complete dissolution of the silver layers and the formation of AgNPs [18]. After cooling to room temperature, the clear X-ray films were removed from the solution, and the AgNPs were recovered by centrifugation, followed by repeated washing with ethanol, dried overnight at 40 °C, and then grounded to powder.

#### *2.2.3 Preparation of humic or fulvic acid-stabilized AgNPs from x-ray films*

The procedure for preparing HA/FA-stabilized AgNPs through the reduction of Ag layers on the X-rays with NaOH as a reducing agent and HA/FA as a capping agent was adapted from previous work [19]. First, 10 g of X-ray films were dispersed in NaOH solution (1.5 M, 100 mL) and heated to 90 °C for 30 min. HA or FA (5 g) was then added to the mixture, and the mixture was heated for an additional 1 h. During this time, the colour changed from grey to dark brown, indicating the successful formation of HA or FA-stabilized AgNPs. The solution was allowed to cool down to room temperature and the clear x-ray films were removed from the solution, and the stabilized AgNPs were recovered by centrifugation, followed by repeated washing with ethanol, and then dried overnight at room temperature to yield powdered HA or FA-stabilized AgNPs.

### 2.3 Material Characterization

Fourier-transform infrared (FTIR) spectroscopy analysis was performed using a Thermo Fisher spectrophotometer with KBr pellet preparation. Sample morphology and elemental composition were characterized by scanning electron microscopy (SEM, XL 30 FEG ESEM) coupled with energy-dispersive X-ray spectroscopy (EDAX). X-ray diffraction (XRD) patterns were obtained using a Rigaku MiniFlex 600 system, with data collection from 5° to 70° 2θ at a scan rate of 1 °/min. Measurements employed a 2.5 s step time, 6.0 mm slit width, and samples mounted on zero-background silicon wafer slides.

### 2.4 Antimicrobial Activity of the Recovered Silver NPs

Six bacterial cultures: Staphylococcus aureus, Pseudomonas aeruginosa, Streptococcus pneumoniae, Klebsiella pneumoniae, Escherichia coli, and Proteus mirabilis were obtained from the Microbiology Laboratory, Federal Polytechnic Ado-Ekiti, Ekiti State, Nigeria. The antimicrobial efficacy of pure and HA- or FA-stabilized AgNPs against the bacterial isolates was investigated using the nutrient agar well diffusion method. The nutrient agar medium was thoroughly mixed to ensure complete dissolution of its components and then sterilized by autoclaving at 120 °C for 15 minutes. After sterilization, the medium was cooled below 50 °C before being dispensed into sterile petri dishes, where it was left to solidify at room temperature before bacterial inoculation. A standardized suspension of each test organism was evenly spread onto the solidified agar plates. Using a sterile 6 mm cork borer, uniform wells were aseptically punched into the agar. Each well was then filled with either pure AgNPs or HA-/FA-stabilized AgNPs at varying concentrations (0.2, 0.4, 0.6,

and 0.8 g per 4 mL distilled water), while distilled water without AgNPs served as the negative control. The plates were incubated for 24 hours at 35 °C, after which the inhibition zones (in millimetres) were measured to determine the antimicrobial activity.

## 3. RESULTS AND DISCUSSION

### 3.1 Scanning Electron Microscopy

The surface imaging and morphological characterization of pure and HA- or FA-stabilized AgNPs were conducted using scanning electron microscopy, with results presented in Figure 1a-b. The SEM image of pure AgNPs shows coarse, distinct aggregates with particles of varying sizes and shapes, clumping together to form large clusters, Figure 1a. Both the HA- and FA-stabilized AgNPs reveal spherical nanoparticles embedded within a network of large organic molecules, displaying flocculent layers and large surface porosity, Figure 1b and c. The HA-stabilized AgNPs appear to be encased in a uniformly spongy, jelly-like organic structure, Figure 1c, while the FA-stabilized AgNPs exhibit smaller, well-distributed nanoparticles with a more clumped appearance, Figure 1b. Similar report has also been documented [20].

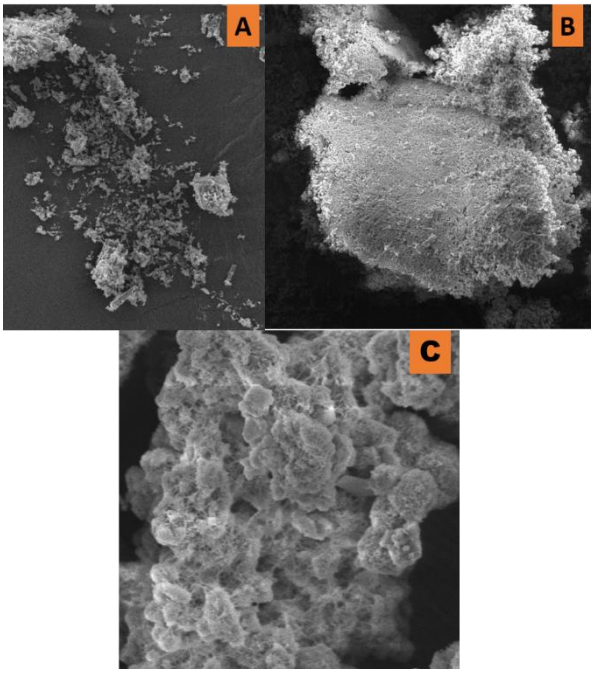


Figure 1: SEM images of (a) bare AgNPs, (b) FA capped AgNPs, and (c) HA capped AgNPs

### 3.2 Functional Group Analysis by FTIR

The surface functionalities of as-synthesized AgNPs and HA/FA-stabilized AgNPs were analysed using FTIR, Figure 2. Pure AgNPs exhibit a broad absorption band around 3450 $cm^{-1}$, indicating the presence of -OH groups from adsorbed water molecules. The FTIR spectra for HA/AgNP and FA/AgNP reveal similar vibrational bands, suggesting that both HA and FA contain similar functional groups. Characteristic bands observed in the spectra of FA/AgNP and HA/AgNP include 3297, 1657, 1555, 1422, 1367, 1180, and 1047 $cm^{-1}$, which correspond to -OH stretching (from phenolic and carboxylic groups), -C=O stretching, -C=C (aromatic conjugated double bond), -C–C (aromatic), CH (aromatic) bending, and C–O stretching vibrations (of ethers, polyols, and esters) [21, 22]. Notably, the FA/AgNP spectrum exhibits more intense vibrational peaks, indicating a higher concentration of oxygen-containing functional groups on its surface compared to HA/AgNP. This suggests slight variations in their structures and implies that FA may have a greater potential to bind with metallic species than HA.

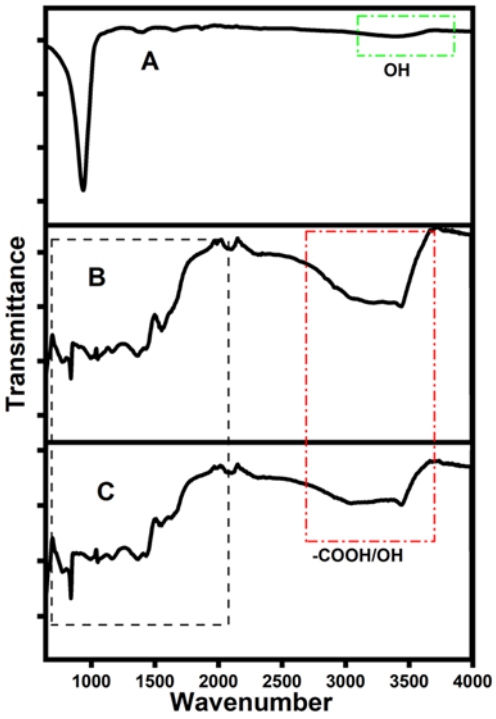


Figure 2: FTIR spectral of (a) bare AgNPs, (b) FA capped AgNPs, and (c) HA capped AgNPs

### 3.2 X-ray Diffractometer (XRD)

The phase crystallinity and formation of the synthesized samples were analysed by powdered XRD, as shown in Figure 3a-c. The x-ray diffraction pattern of pure AgNPs displays high crystallinity, with distinct peaks at 2θ values of 38.4° (111), 44.5° (200), and 64.8° (220). These peaks are also present in the crystal patterns of HA/AgNPs and FA/AgNPs, indicating that the crystal structure of AgNPs is preserved in the composites. Additionally, other sharp diffraction peaks observed in the HA/AgNPs and FA/AgNPs patterns are attributed to inorganic and mineral components within the NOM, such as silica, kaolinite, and calcite. Slight variations in diffraction patterns between HA/AgNPs and FA/AgNPs suggest differences arising from the structural characteristics of HA and FA. Similar report has also been documented [23].

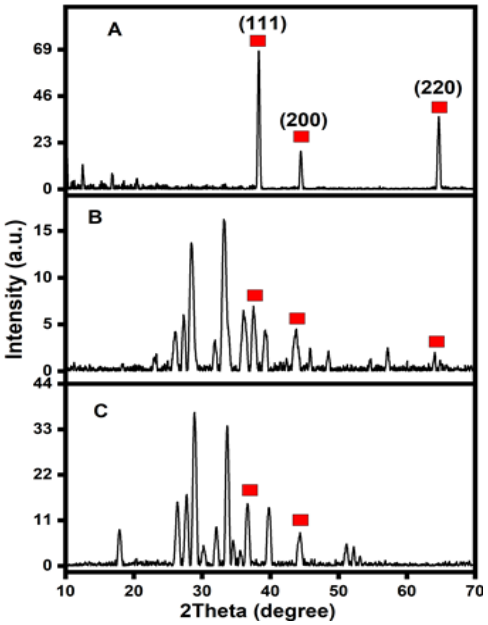


Figure 3: XRD pattern of (a) bare AgNPs, (b) FA capped AgNPs, and (c) HA capped AgNPs

Table 1: Antibacterial activities of fulvic acid/AgNPs from used x-ray film

| Bacterial | Zone of inhibition (mm) | | | | |
|---|---|---|---|---|---|
| | 0.2 g/mL | 0.4 g/mL | 0.6 g/mL | 0.8 g/mL | Control |
| *Escherichia coli* | 10.00 | 13.00 | 18.00 | 30.00 | 0.00 |
| *Pseudomonas aeruginosa* | 11.00 | 15.00 | 15.00 | 18.00 | 0.00 |
| *Klebsiella pneumoniae* | 11.00 | 15.00 | 17.00 | 20.00 | 0.00 |
| *Proteus mirabilis* | 10.00 | 12.00 | 15.00 | 16.00 | 0.00 |
| *Streptococcus pneumoniae* | 34.00 | 30.00 | 37.00 | 39.00 | 0.00 |
| *Staphylococcus aureus* | 9.00 | 15.00 | 18.00 | 20.00 | 0.00 |

Table 2: Antibacterial activities of humic acid/AgNPs from used x-ray film

| Bacterial | Zone of inhibition (mm) | | | | |
|---|---|---|---|---|---|
| | 0.2 g/mL | 0.4 g/mL | 0.2 g/mL | 0.8 g/mL | Control |
| *Escherichia coli* | 25.00 | 25.00 | 30.00 | 35.00 | 0.00 |
| *Pseudomonas aeruginosa* | 13.00 | 20.00 | 28.00 | 25.00 | 0.00 |
| *Klebsiella pneumoniae* | 10.00 | 11.00 | 13.00 | 16.00 | 0.00 |
| *Proteus mirabilis* | 19.00 | 25.00 | 26.00 | 31.00 | 0.00 |
| *Streptococcus pneumoniae* | 12.00 | 15.00 | 16.00 | 20.00 | 0.00 |
| *Staphylococcus aureus* | 18.00 | 21.00 | 25.00 | 27.00 | 0.00 |

Table 3: Antibacterial activities of pure AgNPs from used x-ray film

| Bacterial | Zone of inhibition (mm) | | | | |
|---|---|---|---|---|---|
| | 0.2 g/mL | 0.4 g/mL | 0.2 g/mL | 0.8 g/mL | Control |
| *Escherichia coli* | 11.00 | 12.00 | 14.00 | 16.00 | 0.00 |
| *Pseudomonas aeruginosa* | 13.00 | 16.00 | 15.00 | 20.00 | 0.00 |
| *Klebsiella pneumoniae* | 11.00 | 13.00 | 18.00 | 23.00 | 0.00 |
| *Proteus mirabilis* | 12.00 | 16.00 | 17.00 | 20.00 | 0.00 |
| *Streptococcus pneumoniae* | 10.00 | 12.00 | 14.00 | 19.00 | 0.00 |
| *Staphylococcus aureus* | 16.00 | 11.00 | 19.00 | 25.00 | 0.00 |

### 3.3 Antibacterial Studies

The antibacterial activities of silver nanoparticles (AgNPs) synthesized from used X-ray film reveal significant information into their effectiveness against various bacterial strains. The data illustrate the zones of inhibition (in millimeters) for different concentrations of fulvic acid/AgNPs (Table 1), humic acid/AgNPs (Table 2), and pure AgNPs (Table 3) against several bacterial pathogens, including *E. coli, P. aeruginosa, K. pneumoniae*, *P. mirabilis, S. pneumoniae,* and *S. aureus*.

In Table 1, the antibacterial activities of fulvic acid/AgNPs are presented, showing a notable increase in the zone of inhibition with rising concentrations. For instance, *E. coli* exhibited a zone of inhibition that increased from 10 mm at 0.2 g/mL to 30 mm at 0.8 g/mL. This significant increase confirms the effectiveness of fulvic acid/AgNPs in combating this common pathogen, which is often associated with gastrointestinal infections and other health issues [24]. Similarly, *S. pneumoniae* showed an impressive increase from 34 mm at 0.2 g/mL to 39 mm at 0.8 g/mL (Figure 4), indicating that this formulation is particularly potent against this bacterium. The results indicate that the antibacterial efficacy of these nanoparticles is concentration-dependent, with higher concentrations generally yielding larger zones of inhibition. For instance, the fulvic acid/AgNPs exhibited a maximum zone of inhibition of 39 mm against *Streptococcus pneumoniae* at a concentration of 0.8 g/mL, which is notably higher than the control (0 mm). The results also indicate that while some bacterial strains, such as *P. aeruginosa* and *K. pneumoniae*, displayed moderate increases in inhibition zones, they did not reach the same levels as *E. coli* or *S. pneumoniae*. For instance, *P. aeruginosa* showed a maximum zone of 18 mm at 0.8 g/mL (Table 1 and Figure 4), which is significantly lower than the inhibition observed for *E. coli* and *S. pneumoniae*. This variation in susceptibility may be attributed to differences

in cell wall structure and permeability among the bacterial strains, with Gram-negative bacteria generally exhibiting more resistance due to their outer membrane [25]. This suggests that the combination of fulvic acid with AgNPs enhances their antibacterial properties, likely due to the synergistic effects of the organic compound and the nanoparticles [26].

Table 2 presents the antibacterial activities of humic acid/AgNPs, which also demonstrate a clear concentration-dependent effect. Notably, *Escherichia coli* showed a remarkable inhibition zone of 35 mm at 0.8 g/mL, which is significantly higher than the maximum observed for the same bacterium when treated with fulvic acid/AgNPs. This suggests that humic acid may enhance the antibacterial properties of AgNPs more effectively than fulvic acid in certain contexts. The consistent performance of humic acid/AgNPs across various concentrations indicates its potential as a reliable antimicrobial agent. The performance against *S. aureus* also reflects the effectiveness of humic acid/AgNPs, with inhibition zones increasing from 18 mm at 0.2 g/mL to 27 mm at 0.8 g/mL. This improvement in antibacterial activity with increased concentration aligns with findings from other studies [27, 28]. The ability of humic acid to stabilize AgNPs and enhance their interaction with bacterial cells likely contributes to this observed increase in antibacterial activity [27].

In contrast, humic acid/AgNPs (Table 2) also demonstrate substantial antibacterial activity, with the highest inhibition zone of 35 mm against *E. coli* at 0.8 g/mL (Figure 5). This performance indicates that humic acid, similar to fulvic acid, can effectively stabilize and enhance the antibacterial properties of AgNPs [29, 30]. The comparative analysis of these two types of nanoparticles suggests that while both fulvic and humic acids contribute positively to the antibacterial activity of AgNPs, the specific interactions and mechanisms may differ, warranting further investigation into their respective roles in enhancing AgNP efficacy.

Table 3 illustrates the antibacterial activities of pure AgNPs, which, while effective, show less pronounced increases in inhibition zones compared to the formulations with humic and fulvic acids. For example, *Escherichia coli* exhibited a maximum inhibition zone of only 16 mm at 0.8 g/mL (Figure 6), which is significantly lower than the zones observed with both humic and fulvic acid formulations. This suggests that the presence of organic compounds plays a crucial role in enhancing the antibacterial efficacy of AgNPs. The data for *Staphylococcus aureus* also reflect this trend, with pure AgNPs achieving a maximum inhibition zone of 25 mm at 0.8 g/mL, compared to the 27 mm achieved with humic acid/AgNPs. This indicates that while AgNPs alone possess antibacterial properties, their effectiveness can be significantly enhanced through the use of stabilizing agents like humic and fulvic acids, which may facilitate better dispersion and interaction with bacterial cells.

When examining the pure AgNPs (Table 3 and Figure 6), it is evident that their antibacterial activity is generally lower than that of the formulations with humic or fulvic acid. For example, the maximum zone of inhibition for *S. pneumoniae* is only 25 mm at 0.8 g/mL, which is significantly less than the 39 mm observed with fulvic acid/AgNPs. This disparity shows the importance of the stabilizing agents in enhancing the antibacterial properties of AgNPs [31, 32]. The lower effectiveness of pure AgNPs may be attributed to their tendency to aggregate, which reduces their surface area and, consequently, their interaction with bacterial cells [33].

The findings highlight the potential of using waste materials, such as used X-ray film, as a source for synthesizing AgNPs. This approach not only provides an eco-friendly method for producing antibacterial agents but also addresses waste management issues associated with medical imaging [34, 35]. The utilization of such biogenic synthesis methods can lead to cost-effective and sustainable production of AgNPs, which can be particularly beneficial in developing countries where access to advanced nanotechnology may be limited [36].

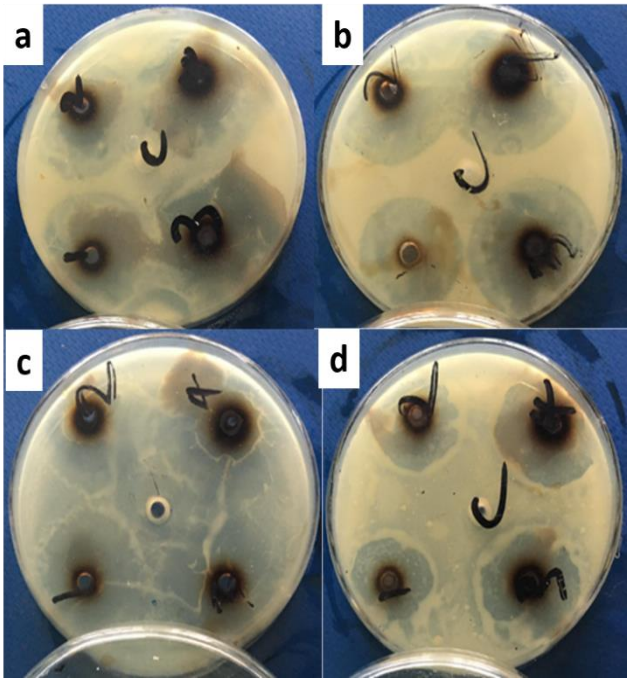


Figure 4: Showing zone of inhibition of varying concentration of fulvic acid/AgNPs from used x-ray film against (a) *K.pneumoniae* (b) *S. aureus* (c) *P. aeruginosa* (d) *E. coli*

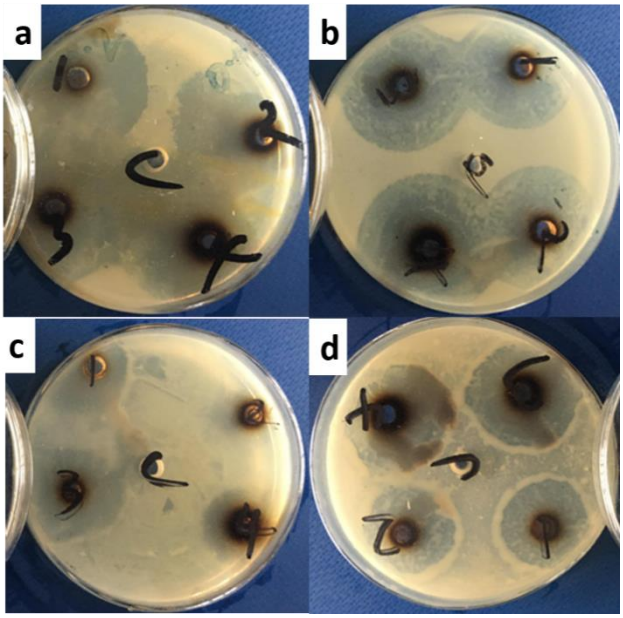


**Figure 5:** Showing zone of inhibition of varying concentration of humic acid/AgNPs from used x-ray film against (a) *K.pneumoniae* (b) *S. aureus* (c) *P. aeruginosa* (d) *E. coli*

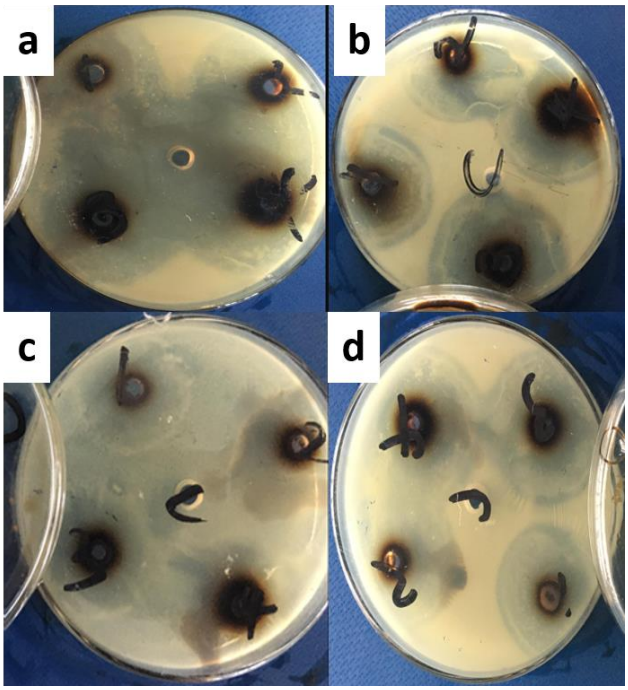


Figure 6: Showing zone of inhibition of varying concentration of AgNPs from used x-ray film against (a) *K.pneumoniae* (b) *S. aureus* (c) *P. aeruginosa* (d) *E. coli*

## 4. CONCLUSION

The recovery and stabilization of AgNPs from used x-ray photographic films offer a sustainable and cost-effective pathway for nanoparticle synthesis with high antimicrobial efficacy. The incorporation of humic acid (HA) and fulvic acid (FA) as stabilizing agents significantly enhanced the biological activity of the AgNPs compared to uncoated AgNPs. The SEM micrographs revealed that HA- and FA-capped AgNPs exhibit a porous structure, which facilitated better interaction with bacterial cells compared to AgNPs. FTIR confirmed the presence of abundant functional groups from HA and FA. XRD analysis showed that while all AgNPs retained their crystalline nature, the HA/FA coatings introduced additional phases linked to the organic stabilizers, which may enhance biocompatibility and interaction with bacterial surfaces. The superior antimicrobial activity of stabilized AgNPs arises from improved surface properties, synergistic action, and enhanced bioavailability. The organic acids themselves possess inherent antimicrobial properties, which synergize with the bactericidal activity of AgNPs, leading to greater inhibition zones. The synthesized AgNPs penetrate bacterial cell walls more efficiently, disrupting cellular functions through mechanisms such as reactive oxygen species generation and membrane damage.

## ACKNOWLEDGMENTS

The authors gratefully acknowledge the University-based research grant/funding, facilities and other institutional support provided by Adekunle Ajasin University, Akungba, Nigeria.

## REFERENCES

[1] Li, X., Li, B., Liu, R., Dong, Y., Zhao, Y. and Wu, Y., 2021. Development of pH-responsive nanocomposites with remarkably synergistic antibiofilm activities based on ultrasmall silver nanoparticles in combination with aminoglycoside antibiotics. *Colloids and Surfaces B: Biointerfaces*, *208*, p.112112.

[2] Patil, A.P., Kapadnis, K.H. and Elangovan, S., 2021. Antibacterial applications of biosynthesized AgNPs: A short review (2015-2020). *Material Science Research India*, *18*(2), pp.143-153.

[3] Lee, S.H. and Jun, B.H., 2019. Silver nanoparticles: synthesis and application for nanomedicine. *International journal of molecular sciences*, *20*(4), p.865.

[4] Xu, L., Wang, Y.Y., Huang, J., Chen, C.Y., Wang, Z.X. and Xie, H., 2020. Silver nanoparticles: Synthesis, medical applications and biosafety. *Theranostics*, 10(20), p.8996.

[5] Barman, K., Chowdhury, D. and Baruah, P.K., 2020. Bio-synthesized silver nanoparticles using Zingiber officinale rhizome extract as efficient catalyst for the degradation of environmental pollutants. *Inorganic and Nano-Metal Chemistry*, *50*(2), pp.57-65.

[6] Adie, G., Shoneye, H. and Iniaghe, P., 2022. Optimizing silver extraction potential from waste x-ray films using acid and alkaline leaching agents. *Annals of Science and Technology*, 7(2), pp.21-28.

[7] Cavello, I., Hours, R. and Cavalitto, S., 2013. Enzymatic hydrolysis of gelatin layers of x-ray films and release of silver particles using keratinolytic serine proteases from

*Purpureocillium lilacinum*. *Journal of Microbiology and Biotechnology*, 23(8), pp.1133-1139.

[8] Al-Abdalall, A. and Al-Khaldi, E., 2016. Recovery of silver from used x-ray film using alkaline protease from *Bacillus subtilis*. *African Journal of Biotechnology*, 15(26), pp.1413-1416.

[9] Shah, P. and Malik, R., 2019. Study of antibacterial activity of *Phyllanthus emblica* and its role in green synthesis of silver nanoparticles. *Journal of Drug Delivery and Therapeutics*, 9(3), pp.76-81.

[10] Nam, S., Hinchliffe, D., Hillyer, M., Gary, L. and He, Z., 2023. Washable antimicrobial wipes fabricated from a blend of nanocomposite raw cotton fiber. *Molecules*, 28(3), p.1051.

[11] Ovais, M., Khalil, A., Raza, A., Khan, M., Ahmad, I., Islam, N. and Shinwari, Z., 2016. Green synthesis of silver nanoparticles via plant extracts: beginning a new era in cancer theranostics. *Nanomedicine*, 11(23), pp.3157-3177.

[12] He, J. and Kappler, A., 2017. Recovery of precious metals from waste streams. *Microbial Biotechnology*, 10, pp.1194-1198.

[13] Urriquia, J.C., Rheinhardt, P.M.C., Tanggol, N.N.T., Gapusan, R., and Balela, M.D.L., 2020. Optimization of silver recovery from waste X-ray radiographic films by oxalic acid extraction with response surface methodology. *Sustainable Chemistry and Pharmacy*, 17, p.100294.

[14] Iravani, S., Korbekandi, H., Mirmohammadi, S.V. and Zolfaghari, B., 2014. Synthesis of silver nanoparticles: chemical, physical and biological methods. *Research in Pharmaceutical Sciences*, 9(6), pp.385-406. PMID: 26339255.

[15] Rafique, M., Sadaf, I., Rafique, M.S. and Tahir, M.B., 2017. A review on green synthesis of silver nanoparticles and their applications. *Artificial Cells, Nanomedicine, and Biotechnology*, 45, pp.1272-1291.

[16] Dharejo, S.A., Pirzada, T., Shah, M.R., Nadeem, A. and Thebo, K.H., 2025. In-vitro study of hybrid silver nanoparticles with humic acid extracted from cow dung against pathogens. *Heliyon*, 11(1), p.e41636.

[17] Rodríguez-Félix, F., Graciano-Verdugo, A., Moreno-Vásquez, M., Lagarda-Díaz, I., Barreras-Urbina, C., Armenta-Villegas, L. and Tapia-Hernández, J., 2022. Trends in sustainable green synthesis of silver nanoparticles using agri-food waste extracts and their applications in health. *Journal of Nanomaterials*, 2022(1).

[18] Soja, S.F., Wiwi, S., Ali, K. and Fikri, A.S., 2020. Silver recovery from X-ray film waste by leaching and precipitation method using sodium hydroxide and sodium sulfide. *Jurnal Kimia Valensi*, 6(1), pp.62-69.

[19] Dubas, S.T. and Pimpan, V., 2008. Humic acid assisted synthesis of silver nanoparticles and its application to herbicide detection. *Materials Letters*, 62(17-18), pp.2661–2663.

[20] Akintelu, S., Folorunso, A. and Ademosun, O., 2019. Instrumental characterization and antibacterial investigation of silver nanoparticles synthesized from *Garcinia kola* leaf. *Journal of Drug Delivery and Therapeutics*, 9(6-s), pp.58-64.

[21] Singh, K., Naidoo, Y., Mocktar, C. and Baijnath, H., 2018. Biosynthesis of silver nanoparticles using *Plumbago auriculata* leaf and calyx extracts and evaluation of their antimicrobial activities. *Advances in Natural Sciences: Nanoscience and Nanotechnology*, 9(3), p.035004.

[22] Agnihotri, S., Mukherji, S. and Mukherji, S., 2014. Size-controlled silver nanoparticles synthesized over the range 5–100 nm using the same protocol and their antibacterial efficacy. *RSC Advances*, 4(8), pp.3974-3983.

[23] Rousta, M. and Ghasemi, N., 2019. Green synthesis of silver nanoparticles using a mountain plant extract. *Revue Roumaine de Chimie*, 64(2), pp.143-152.

[24] Gifardi, M., Sutardi, L., Farida, W., Prawira, A. and Agungpriyono, S., 2022. Antibacterial activity of Sunda porcupine quill extract (*Hystrix javanica*) against *Staphylococcus aureus*. *Biodiversitas Journal of Biological Diversity*, 23(8), pp.4355-4360.

[25] Lai, C., 2018. Facile formation of colloidal silver nanoparticles using electrolysis technique and their antimicrobial activity. *Micro & Nano Letters*, 13(3), pp.407-410.

[26] Adegboyega, N., Sharma, V., Šišková, K., Zbořil, R., Sohn, M., Schultz, B. and Banerjee, S., 2012. Interactions of aqueous Ag+ with fulvic acids: mechanisms of silver nanoparticle formation and investigation of stability. *Environmental Science & Technology*, 47(2), pp.757-764.

[27] Haqq, S., Pandey, H., Gerard, M. and Chattree, A., 2018. Bio-fabrication of silver nanoparticles using *Chrysanthemum coronarium* flower extract and its in vitro antibacterial activity. *International Journal of Applied Pharmaceutics*, 10(5), pp.209-213.

[28] Budaraga, I., Putra, D. and Wellyalina, W., 2020. Antibacterial activity of moringa leaf layer cake against *S. aureus* and *E. coli*. *Journal of Applied Agricultural Science and Technology*, 4(1), pp.56-63.

[29] Lopez, E., Zafra, M., Gavan, J., Villena, E., Almaquer, F. and Perez, J., 2020. Humic acid functionalized-silver nanoparticles as nanosensor for colorimetric detection of copper (II) ions in aqueous solutions. *Key Engineering Materials*, 831, pp.142-150.

[30] Lopez, E., Zafra, M., Gavan, J., Villena, E. and Perez, J., 2023. Effect of ligand concentration on the stability and copper (II) sensing performance

of humic acid-functionalized silver nanoparticles. *Materials Science Forum*, 1090, pp.81-90.

[31] Niska, K., Knap, N., Kędzia, A., Jaśkiewicz, M., Kamysz, W. and Inkielewicz-Stępniak, I., 2016. Capping agent-dependent toxicity and antimicrobial activity of silver nanoparticles: an in vitro study. *International Journal of Medical Sciences*, 13(10), pp.772-782.

[32] Abdellatif, A., Alturki, H. and Tawfeek, H., 2021. Different cellulosic polymers for synthesizing silver nanoparticles with antioxidant and antibacterial activities. *Scientific Reports*, 11(1), p.84.

[33] Phú, Đ., Quốc, L., Duy, N., Lan, N., Du, B., Luân, L. and Hiến, N., 2014. Study on antibacterial activity of silver nanoparticles synthesized by gamma irradiation method using different stabilizers. *Nanoscale Research Letters*, 9(1), p.162.

[34] Dong, F. and Li, S., 2018. Wound dressings based on chitosan-dialdehyde cellulose nanocrystals-silver nanoparticles: mechanical strength, antibacterial activity and cytotoxicity. *Polymers*, 10(6), p.673.

[35] Lateef, A., Akande, M., Ojo, S., Folarin, B., Kana, E. and Beukes, L., 2016. Paper wasp nest-mediated biosynthesis of silver nanoparticles for antimicrobial, catalytic, anticoagulant, and thrombolytic applications. *3 Biotech*, 6(2), p.140.

[36] Feng, D., Zhang, R., Zhang, M., Fang, A. and Shi, F., 2022. Synthesis of eco-friendly silver nanoparticles using glycyrrhizin and evaluation of their antibacterial ability. *Nanomaterials*, 12(15), p.2636.